



Original Research

Nafamostat mesylate overcomes endocrine resistance of breast cancer through epigenetic regulation of CDK4 and CDK6 expression

Yueh-Te Lin ^{a,1}, Joseph Lin ^{b,d,1}, Yi-En Liu ^c, Kai-Wen Hsu ^e, Chang-Chi Hsieh ^d, Darren Chen ^{b,c,f,**}, Han-Tsang Wu ^{c,*}

^a Cancer Genome Research Center, Chang Gung Memorial Hospital at Linkou, Gueishan Dist., Taoyuan 333, Taiwan

^b Comprehensive Breast Cancer Center, Changhua Christian Hospital, Changhua 500, Taiwan

^c Cancer Research Center, Changhua Christian Hospital, Changhua 500, Taiwan

^d Department of Animal Science and Biotechnology, Tunghai University, Taichung 407, Taiwan

^e Research Center for Cancer Biology, Institute of New Drug Development, China Medical University, Taichung 404, Taiwan

^f School of Medicine, Chung Shan Medical University, Taichung 402, Taiwan



ARTICLE INFO

Keywords:

Endocrine resistance
Estrogen receptor-positive breast cancer
Nafamostat mesylate
CDK4/6

ABSTRACT

Breast cancer is common worldwide, and the estrogen receptor-positive subtype accounts for approximately 70% of breast cancer in women. Tamoxifen and fulvestrant are drugs currently used for endocrinal therapy. Breast cancer exhibiting endocrine resistance can undergo metastasis and lead to the death of breast cancer patients. Drug repurposing is an active area of research in clinical medicine. We found that nafamostat mesylate, clinically used for patients with pancreatitis and disseminated intravascular coagulation, acts as an anti-cancer drug for endocrine-resistant estrogen receptor-positive breast cancer (ERPBC). Epigenetic repression of CDK4 and CDK6 by nafamostat mesylate induced apoptosis and suppressed the metastasis of ERPBC through the deacetylation of Histone 3 Lysine 27. A combination of nafamostat mesylate and CDK4/6 inhibitor synergistically overcame endocrine resistance in ERPBC. Nafamostat mesylate might be an essential adjuvant or alternative drug for the treatment of endocrine-resistant ERPBC due to the low cost-efficiency of the CDK4/6 inhibitor.

Introduction

Breast cancer (BC) is the most common cancer among women worldwide. Approximately 70% of BCs are estrogen receptor (ER)/progesterone receptor-expressing tumors in which hormones play a pivotal role in receptor activation, which triggers the growth and progression of the cancer cells. The receptor status has been used as a biomarker for therapy and prognosis. Current guidelines from the American Society of Clinical Oncology and the College of American Pathologists recommend that tumor specimens with at least 1% of cancer nuclei which stain for the marker are considered to be ER-positive [1]. Presently, ER-positive BC (ERPBC) patients are treated with endocrine therapy that antagonizes the estrogen signals. This approach remains the backbone of therapy, since its efficacy is at least

equal to that of chemotherapy, and it has a better toxicity profile [2].

Earlier randomized trials have indicated that the use of endocrine therapies significantly lowers the recurrence and mortality rates of ERPBC [3]. Tamoxifen is a non-steroidal selective ER modulator (SERM) with mixed ER agonist and antagonist activities, and has been used widely over the past three decades. It remains important, because 67% of BC patients respond to tamoxifen as the first-line therapy [4]. However, approximately 20% of patients diagnosed with operable ER-positive tumors experience recurrent metastatic disease, in which the development of resistance to endocrine therapy is frequently observed [5]. Several mechanisms of endocrine resistance have been identified, including aberrations in the ER/PR pathway, ESR1 gene mutations, increased receptor tyrosine kinase signaling, post-translational modification, and altered cell cycle regulation [6].

Abbreviations: BC, breast cancer; EMT, epithelial-mesenchymal transition; ER, estrogen receptor; ERPBC, estrogen receptor-positive breast cancer; MMP, mitochondrial membrane potential; NM, nafamostat mesylate; PFS, progression-free survival; SERD, selective estrogen receptor degrader; SERM, selective ER modulator.

* Corresponding author.

** Corresponding author at: Comprehensive Breast Cancer Center, Changhua Christian Hospital, Changhua 500, Taiwan.

E-mail addresses: darren.chen@cch.org.tw (D.-R. Chen), 182033@cch.org.tw (H.-T. Wu).

¹ These authors contributed equally to this work.

<https://doi.org/10.1016/j.tranon.2021.101302>

Received 25 November 2021; Accepted 29 November 2021

1936-5233/© 2021 The Authors. Published by Elsevier Inc. This is an open access article under the CC BY-NC-ND license

(<http://creativecommons.org/licenses/by-nc-nd/4.0/>).

This heterogeneity in the development of resistance has an impact not only on the disease progression, but also on the therapeutic strategies used, since an earlier study showed that ESR1 mutations confer resistance to aromatase inhibitor (AI) but not to fulvestrant [7]. Fulvestrant is a selective estrogen receptor degrader (SERD) administered in metastatic ERPC as both a first and second line therapy. SERD is as effective as AI in the first-line setting as a monotherapy, but drug-resistance inevitably develops, as it does in other endocrine therapies [8].

Nafamostat mesylate (NM) is a synthetic serine protease inhibitor used for patients with pancreatitis, disseminated intravascular coagulation, and systematic inflammatory response syndrome [9,10]. NM acts through the inhibition of nuclear factor kappa B (NF- κ B), a transcriptional factor that binds the promoter of the immunoglobulin kappa chain in B cells, causing further apoptosis of pancreatic cancer cells [11, 12]. A recent investigation reported that NM treatment inhibits cyclin-dependent kinase 1 (CDK1), further reducing the proliferation, migration, and invasion of human triple-negative BC cell lines [13]. The safety of high doses of NM has been determined, and it has been approved as a therapeutic drug. It has been demonstrated to have anti-cancer activity when combined with chemotherapy or other anti-cancer therapeutic agents [13,14].

Epigenetic regulation refers to functional changes associated with histone modification, DNA methylation, and noncoding RNAs [15,16]. Histone modification is governed by acetylation, methylation, phosphorylation, ubiquitination, etc. For histone acetylation, two groups of enzymes that have opposing effects: histone acetyltransferases (HATs) and histone deacetylases (HDACs). HATs acetylate the lysine residues in the core histone, leading to more transcriptionally active chromatin. HDACs remove the acetyl group, which suppresses gene expression [15, 17].

In the present study, we sought to identify whether this low toxicity serine protease inhibitor could be used chemotherapeutically to treat and prevent the metastasis of endocrine resistance in ERPC cells. The potential functions and mechanisms of NM were evaluated, with particular emphasis on the suppression of the proliferation and metastasis of the ERPC cells.

Materials and methods

Cell culture

Tamoxifen-resistant (MCF7-TamR) was purchased from Merck (Dietikon, Switzerland), fulvestrant-resistant (MCF7-TamR) was purchased from AXOL (Cambridge, United Kingdom), parental ER+ breast cell lines [MCF7-Control (Ctrl)] and T47D were purchased from the American Type Culture Collection (ATCC, Manassas, VA, USA). T47D was treated with tamoxifen (Sigma, St. Louis, MO, USA) or fulvestrant (Cayman Chemical, East Ellsworth Rd., MI, USA) and selected resistance cells, T47D-TamR and T47D-FulR, respectively. MCF7-TamR and MCF7-FulR cells were cultured in DEME/F12 medium with low glucose and 1% of FBS containing 1 μ M of tamoxifen or 0.1 μ M fulvestrant. MCF7 and T47D cells were cultured in DMEM (Dulbecco's modified Minimal Essential Medium) medium with high glucose and 10% of FBS. T47D-TamR and T47D-FulR were cultured in DMEM with high glucose and 10% of FBS containing 1 μ M of tamoxifen or 0.1 μ M fulvestrant. The human normal breast cell line, H184B5F5/M10 was obtained from the Bioresource Collection and Research Center (Hsinchu, R.O.C). H184 cells were cultured in MEM-alpha medium with 10% FBS.

Cell cytotoxicity assay

Cell cytotoxicity was determined using the 3-(4,5-dimethylthiazol-2-yl)-2,5-diphenyltetrazolium bromide (MTT) assay. For the effect of nafamostat mesylate on MCF7-TamR, MCF7-FulR, MCF7 cell lines were seeded in 96-well plates, treated with various concentrations of nafamostat mesylate (30, 60, and 90 μ M) for 72–96 h. The medium was

removed, and 30 μ L of MTT (Sigma-Aldrich, St. Louis, MO, USA) at 0.5 mg/mL was added to the wells and then incubated at 37 °C for 3–4 h. The blue formazan crystals that formed were dissolved in DMSO, and the absorption was measured at 595 nm using an ELISA plate reader. For the combinational effect of nafamostat mesylate with CDK4/6 inhibitors palbociclib [Cayman Chemical (East Ellsworth Rd., MI, USA)], MCF7-TamR and MCF7-FulR cells were seeded in 96-well plates overnight followed by treatment with nafamostat mesylate (20 μ M) and palbociclib (10 μ M) for 72–96 h. The following process was described similarly as above.

Colony formation assay

Cells were seeded in 12-well plates and then treated with various concentrations of nafamostat mesylate or combined with palbociclib for 48 h. Media were changed every 3 days. After 14–21 days, cells were washed with PBS and fixed with methanol at 25 °C for 15 min. The fixed cells were then stained with 0.5% crystal violet (Sigma, St. Louis, MO, USA) for 35 min, washed with water, and then air-dried. Images were obtained using a digital camera. Absorption was measured at 550 nm using an ELISA plate reader. The crystal violet was dissolved by solution (33% acetic acid).

Apoptosis analysis

Cells were seeded in 12-well plates overnight, treated with various concentrations of nafamostat mesylate or combined with palbociclib for 96 h, and harvested after removing the medium. The harvested cells were incubated with Muse™ Annexin-V & Dead Cell kit reagent (Merck Millipore, Billerica, MA, USA) at 25 °C for 20 min in the dark. The apoptotic cells were measured using a Muse™ Cell Analyzer (Merck Millipore, Billerica, MA, USA), and data were analyzed using MUSE 1.5 Analysis software (Merck Millipore, Billerica, MA, USA).

Mitochondrial membrane potential analysis

Cells were seeded in 12-well plates overnight, treated with various concentrations of nafamostat mesylate or combined with palbociclib for 72 h, and harvested after removing the medium. The harvested cells were resuspended in Muse™ MitoPotential Kit reagent (Merck Millipore, Billerica, MA, USA), and cells were incubated at 37 °C for 20 min. 7-AAD was added, and cells were incubated at 25 °C for 5 min. The mitochondrial membrane potential of cells was determined using the Muse™ Cell Analyzer (Merck Millipore, Billerica, MA, USA), and data were analyzed using MUSE 1.5 Analysis software (Merck Millipore, Billerica, MA, USA).

Protein extraction and Western blot analysis

The method for protein extraction and Western blot analysis were described previously [15,18]. For extraction of proteins from cell lines, RIPA buffer (50 mM Tris pH 7.5, 1% NP-40, and 0.1% SDS) containing protease inhibitors were used. Cell lysates were extracted by centrifugation at 13,000 rpm. at 4 °C for 10 min. The protein content in the supernatants was determined using the Bradford method (Bio-Rad Laboratories). For Western blot analysis, 15–50 mg of cell lysates from each cell line with/without nafamostat mesylate or combined with palbociclib were loaded to 8–12% SDS-PAGE gels and transferred to nitrocellulose membranes (GE Healthcare Life Science). The membranes were incubated with antibodies overnight at 4 °C. The antibodies used in these studies are listed in supplementary Table 1. Signals were detected using an ECL chemiluminescence kit (GE Healthcare Life Science, Little Chalfont, Bucks, UK).

RNA extraction and quantitative real-time PCR analysis

TRI Reagent (Sigma, St. Louis, MO, USA) was used for RNA extraction from cell lines. The quantitative real-time PCR analysis was performed in a PRISM ABI7700 Sequence Detection System (Applied Biosystems, Foster City, CA, USA) with the preset PCR program, and 18 s rRNA was selected as an internal control. cDNA (10 ng) and primers (200 nM) were used for the reaction in 1X SYBR Green Mixture (Kapa Biosystems, Woburn, MA USA) in a total volume of 20 μ L. The sequences of the primers used in the quantitative real-time PCR experiment are listed in supplementary Table 2.

qChIP real-time PCR analysis

The method for qChIP real-time PCR analysis were described previously [15,18]. Cells were seeded in 10 cm cell culture dishes overnight, treated with various concentrations of nafamostat mesylate for 48–72 h, cross-linked with 1% formaldehyde for 10 min, and stopped by adding glycine to a final concentration of 0.125 M. Fixed cells were washed twice with Tris-buffered saline (20 mM Tris, pH 7.5, and 150 mM NaCl) and harvested in 2 mL of PBS buffer with protease inhibitors. Cells were pelleted by centrifugation and suspended in 200 mL of RIPA buffer. Cells were sonicated with a 0.25-inch diameter probe for 15 s twice using a Bioruptor® Pico sonicator (Diagenode, Belgium). For each immunoprecipitation, 500 μ L of lysate was pre-cleared by adding 50 μ L of blocked protein A beads (50% protein A-Sepharose, Amersham Biosciences; 0.5 mg mL⁻¹ bovine serum albumin, 0.2 mg mL⁻¹ salmon sperm DNA) at 4 °C for 1 h. Samples were spun, and the supernatants were incubated at 4 °C for 3 h with no antibody, nonspecific IgG, or antibodies to be tested. Immune complexes were recovered by adding 50 mL of blocked protein A beads and incubated at 4 °C overnight. DNA fragment extraction from beads was performed using the Chromatin Immunoprecipitation (ChIP) assay kit (Merck Millipore, Billerica, MA, USA). For qChIP-real-time PCR analysis, DNA samples were quantified by the SYBR Green assay using 1X SYBR Green Mixture (Kapa Biosystems, Woburn, MA, USA) with specific primers in a total volume of 20 μ L. Data were analyzed by the CT method and plotted as % input DNA. qChIP values were calculated by the following formula: % input recovery = [100/(input fold dilution/bound fold dilution)] \times 2^(input CT-b_ound CT). The antibodies used in qChIP-real-time PCR analysis are listed in Table 1. The primers used in qChIP real-time PCR analysis are listed in supplementary Table 2.

Statistical analysis

All error bars analysis was assessed by STDEV. The Student's *t*-test analysis was used to compare untreated cells. The one-way ANOVA analysis was used to compare between different groups under the same concentration. Each data is presented as mean SEM.

In-vivo xenograft studies

All animal work was carried out in accordance with The AAALAC international for animal care. Eight-week-old female SCID mice (NLAC, Taiwan) were housed under specific pathogen-free conditions and provided with food and water ad libitum. We numbered mammary ducts 1–10 in the female mice (Fig. 8A). On day 0, orthotopic mammary tumors were inoculated with the breast tumor cell line MCF7-TamR and MCF7-FulR (10 \times 10⁶ cells in Matrigel) at mammary duct 4 or 9 (Fig. 8A). Tumors were measured twice a week with digital microcalipers and volumes calculated (volume \times (width² \times length)/2). The average tumor volume reached 50–100 mm³ on day 32. The mice were then injected with nafamostat mesylate at a concentration of 30 mg kg⁻¹ per mouse (*n* = 6) intraperitoneally, and six mice were kept saline treatment as a control (*n* = 6). Tumors were measured twice weekly, and once the maximal tumor volume was reached (400–600 mm³), mice

were sacrificed. Tumor volumes are represented as mean volume \pm s.d.

Immunohistochemistry and nucleus staining analysis

Immunohistochemistry staining analysis was performed by using Mouse and Rabbit Specific HRP/DAB IHC Detection Kit - Micro-polymer (Abcam) and anti-CDK4 and CDK6 antibodies. (B) The nucleus staining analysis was performed by counting DAB-positive nucleus staining in random nine IHC images.

Cell cycle analysis

Cells were seeded in 6 cm dish, starvation overnight, and then treated with various concentrations of nafamostat mesylate for 24 h, and then the cells were collected after removing the medium. The collected cells were first fixed in 70% ethanol (Sigma-Aldrich, St. Louis, MO, USA) at –20 °C for 16–18 h. The 70% ethanol was removed, and the fixed cells were suspended in Muse™ Cell Cycle Kit (Merck Millipore, Billerica, MA, USA) at 25 °C for 30 min in the dark. The distribution of the cell cycle was measured by Muse™ Cell Analyzer (Merck Millipore, Billerica, MA, USA), and data were analyzed by MUSE 1.5 Analysis software (Merck Millipore, Billerica, MA, USA).

Results

Nafamostat mesylate induced the apoptosis of endocrine-resistant ERPBCs

Normal breast epithelial cells (H184) were first assessed to clarify whether nafamostat mesylate (NM) is a potential anti-cancer drug for estrogen receptor-positive breast cancer (ERPBC) since the side-effect of NM on normal human cells should be assessed. The viability of H184 cells was slightly reduced at a higher dose (90 and 120 μ M) of NM (Fig. 1A). However, NM did not affect the viability of ERPBC (MCF7 and T47D) cells (Fig. 1B and supplementary Fig. 1A). We further evaluated whether NM is a potential drug for overcoming the endocrine resistance of ERPBC. Both Tamoxifen- and fulvestrant-resistant ERPBC cells (MCF7-TamR and MCF7-FulR) were treated with a serial dose of NM for 72 and 96 h. The viability of MCF7-TamR and -FulR cells was significantly inhibited by NM in a dose and time-dependent manner (Fig. 1B). The similar result was also observed in another ERPBC cell line with endocrine resistance (supplementary Fig. 1A and B). The proliferation of MCF7-TamR and MCF7-FulR cells was also significantly decreased by a serial dose (30 to 90 μ M) of NM (Fig. 1C and D). NM also caused significant apoptosis of MCF7-TamR and MCF7-FulR cells in a dose-dependent manner (Fig. 2A and B). The levels of cleaved caspase-related proteins, such as cleaved PARP, caspase 3, caspase-7, and caspase 9, were increased in MCF7-TamR and MCF7-FulR cells under serial doses of NM (Fig. 2C). Depolarization of the mitochondrial membrane potential (MMP) was markedly increased by NM in a dose-dependent manner, compared with untreated MCF7-TamR and -FulR cells, since disruption of the MMP is related to apoptosis (Fig. 2D and E). The protein levels of members of the Bcl-related families and death families were also investigated in MCF7-TamR and -FulR cells treated with a serial dose of NM. The levels of Bim and BAX protein were increased, and those of Bcl-2 and Bcl-XL were decreased (Fig. 2F).

Nafamostat mesylate suppressed metastasis of endocrine-resistant ERPBCs

Drug-resistant cancer cells often have enhanced metastatic activity and higher aggressive proliferation ability [19]. The migration and invasion abilities of MCF7-TamR and MCF7-FulR cells following 30 μ M of NM treatment for 18 h were assessed using *in vitro* Transwell migration and invasion assays. The migration activity of MCF7-TamR and MCF7-FulR cells was significantly decreased by treatment with 30 μ M of NM (Fig. 3A and B). The invasive activity of MCF7-TamR and MCF7-FulR cells was also significantly repressed by NM (Fig. 3C and D).

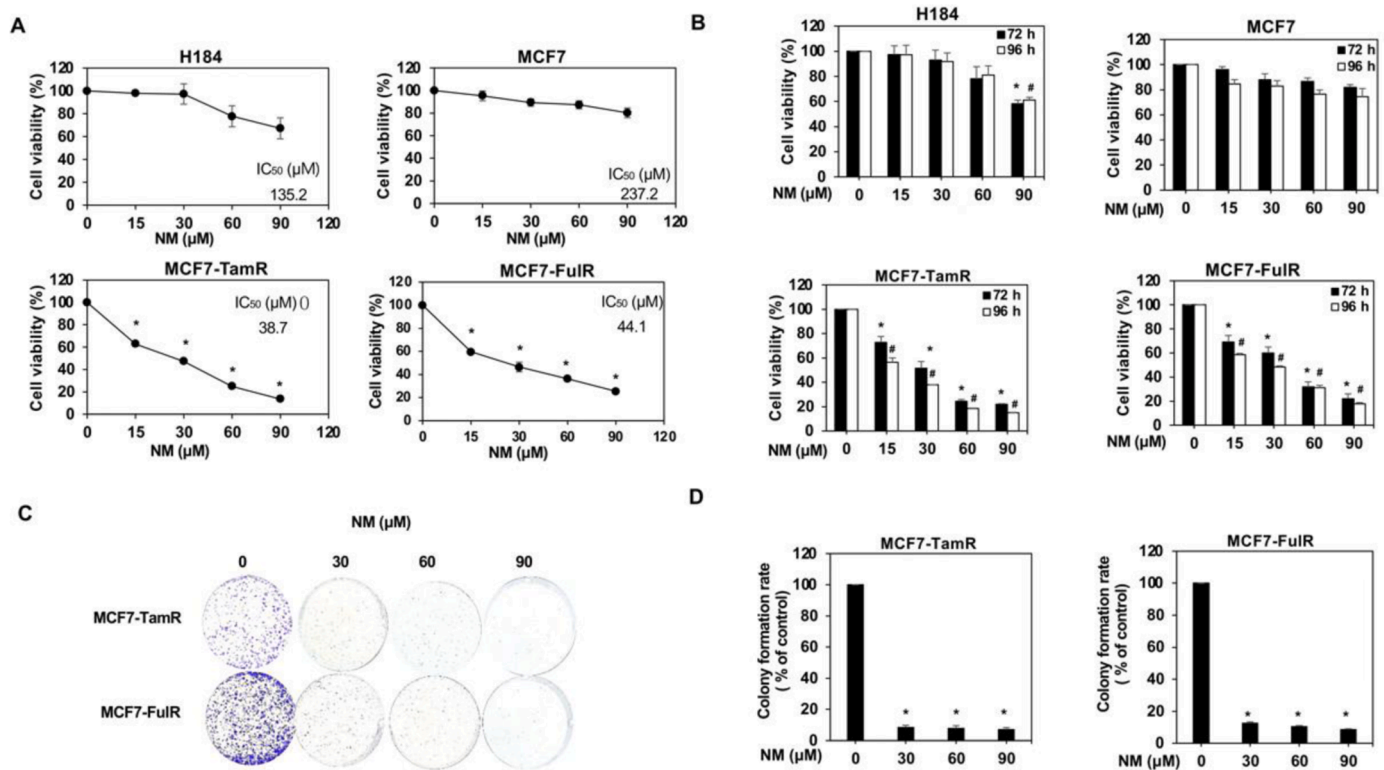


Fig. 1. Inhibitory effect of nafamostat mesylate on cell viability of endocrine-resistant estrogen receptor-positive breast cancer. (A) IC₅₀ values of H184, parental MCF7, MCF7-TamR, and MCF7-FulR cells for NM. (B) Analysis of the viability of H184, parental MCF7, MCF7-TamR and -FulR cells treated with various doses of NM for 72 and 96 h, using MTT assays. (C) Analysis of growth of MCF7-TamR (upper) and MCF7-FulR (lower) cells, assessed using colony formation assays. (D) Quantitative analysis of colony formation assays for NM-treated MCF7-TamR (left) and MCF7-FulR (right) cells. Data are represented as the mean ± SEM for biological triplicate experiments. *[#]*P* < 0.01, compared with the results for untreated H184, parental MCF7, MCF7-FulR, and MCF7-TamR cells.

The levels of epithelial-mesenchymal transition (EMT)-related proteins were evaluated in MCF7-TamR and MCF7-FulR cells treated with serial doses of NM, using western blotting. The levels of the epithelial markers E-cadherin and B-catenin were increased, whereas the levels of the mesenchymal markers N-cadherin and vimentin were decreased (Fig. 3E).

Nafamostat mesylate epigenetically repressed CDK4 and CDK6 expressions in endocrine-resistant ERPCs

NM appears to be a promising anti-cancer drug for overcoming endocrine resistance in ERPC. Drugs inhibiting CDK4/6 activity, such as palbociclib, have been widely used as therapeutic strategies for ERPC patients with endocrine resistance [20]. However, the high cost of palbociclib (PAL) is a problem, and the mortality rates are still high [21]. Therefore, the exploration of alternative strategies to combat endocrine resistance in ERPC is essential. Hence, the levels of members of the CDK families were evaluated in MCF7-TamR and MCF7-FulR cells treated with NM, using western blot analysis. Serial doses of NM administered to MCF7-TamR and MCF7-FulR cells produced significant decreases in the protein levels of CDK4 and CDK6, but not CDK1 or CDK2 (Fig. 4A). The mRNA levels of CDK4 and CDK6 were decreased by NM in two different lines of endocrine drug-resistant ERPC cells (Fig. 4B). Histone acetylation is related to gene expression [22]. The levels of acetylated lysines 9, 27, and 56 of Histone 3 were evaluated in MCF7-TamR and MCF7-FulR cells under treatment with serial doses of NM. Only the acetylation of Histone 3 Lysine 27 was downregulated by NM in two different endocrine drug-resistant ERPC cells (Fig. 4C). The localization of H3K27Ac on the promoter region of CDK4 and CDK6 was further evaluated in NM-treated MCF7-TamR and MCF7-FulR cells using qChIP-PCR experiments. A decrease in the binding levels of H3K27Ac on

the promoter region of CDK4 and CDK6 was consistently observed in two different hormonal drug-resistant ERPC cells treated with serial doses of NM (Fig. 4D–F). CDK4 and CDK6 activity has been reported to be linked to tumor progression and cancer metastasis [23]. Besides, no specific and consistent effect on the binding levels of H3K27Ac on the promoter region of two housekeeping genes (GAPDH and β-actin) and other CDK family members (CDK1 and CDK2) was observed in NM-treated MCF7-TamR and MCF7-FulR cell (Supplementary Fig. 4A–C). FACS analysis for cell cycle progression in MCF7-TamR and -FulR cells under serial doses of NM treatment was performed. The result indicated G1/S arrest was observed in NM-treated MCF7-TamR and MCF7-FulR cells in a dose-dependent manner (supplementary Fig. 2A and B). Moreover, phosphorylated Rb, a substrate for CDK4/6, was downregulated by NM in MCF7-TamR and -FulR cells (supplementary Fig. 3B). The CDK4 and CDK6 expressions were evaluated in H184, MCF7-TamR, and MCF7-FulR by western blot analysis. The result showed a higher expression of CDK4 in MCF7-TamR and MCF7-FulR cells compared with H184 cells and MCF7 cells (supplementary Fig. 3A). Besides, CDK6 expression in MCF7-TamR and MCF7-FulR cells was higher than in MCF7 cells (supplementary Fig. 3A). Taken together, these results indicate that NM may induce apoptosis and suppress metastasis in endocrine-resistant ERPCs via the epigenetic down-regulation of CDK4 and CDK6 expression.

Enhanced induction of apoptosis and suppression of the metastasis in endocrine-resistant ERPCs by combinational treatment of nafamostat mesylate and CDK4/6 inhibitor

NM represses CDK4 and CDK6 expression in endocrine-resistant ERPCs, and the use of combinations of anti-cancer drugs in the treatment of various types of cancer is an emerging issue in clinical medicine

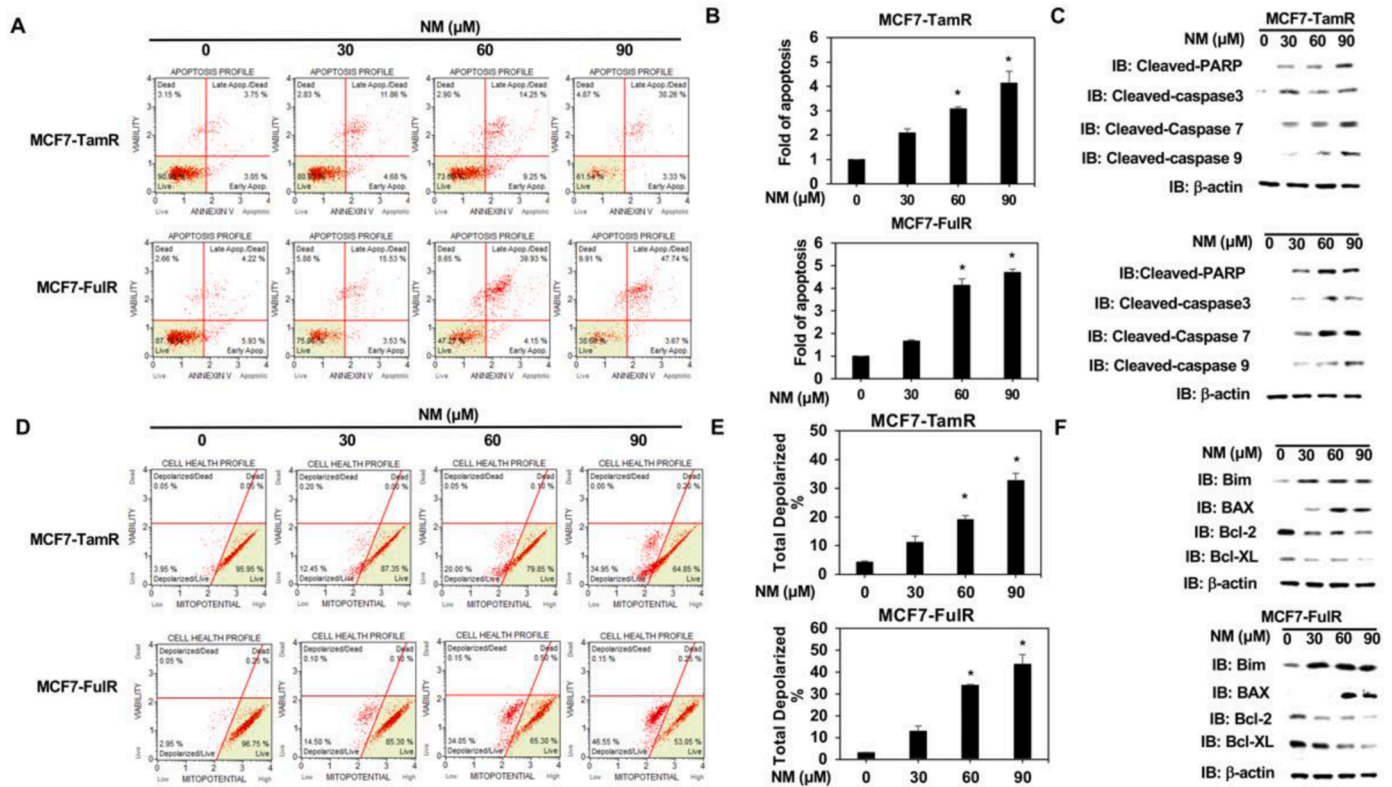


Fig. 2. Effect of nafamostat mesylate on apoptosis of endocrine-resistant estrogen receptor-positive breast cancer cells. (A) Analysis of apoptosis in MCF7-TamR (upper) and MCF7-FulR (lower) cells treated with serial doses of NM, assessed by Annexin V-dependent flow cytometry assays. (B) Quantitative analysis of apoptotic levels of serial doses of NM-treated MCF7-TamR (upper) and FulR (lower) cells (C) Levels of cleaved caspase family members in MCF7-TamR (upper) and FulR (lower) cells under serial doses of NM, assessed by western blot analysis using specific antibodies. (D) Analysis of mitochondrial membrane potential for MCF7-TamR (upper) and MCF7-FulR (lower) cells treated with serial doses of NM, assessed using flow cytometry assay. (E) Quantitative analysis of total depolarized levels of serial doses of NM-treated MCF7-TamR (upper) and FulR (lower) cells (F) Levels of BCL families and death signaling-related proteins in MCF7-TamR (upper) and FulR (lower) cells under serial doses of NM, assessed using western blot analysis with specific antibodies. Data are represented as the mean ± SEM for biological triplicate experiments. **P* < 0.01, compared with the results for untreated MCF7-FulR and MCF7-TamR cells.

[24]. We, therefore, evaluated the use of combined NM and PAL, a CDK4/6 inhibitor, for overcoming endocrine resistance in ERPBCs. The IC₅₀ values of MCF7-TamR and MCF7-FulR cells for PAL were 24.9 and 15.2 μM, respectively (Fig. 5A). The lower dose of NM (20 μM) and PAL (10 μM) was used in combination to assess the effect of this strategy on the apoptosis of MCF7-TamR and MCF7-FulR cells. The viability of MCF7-TamR and MCF7-FulR cells was synergistically inhibited by combination treatment with NM and PAL (Fig. 5B). Cotreatment with NM and PAL also synergistically caused apoptosis of MCF7-TamR and MCF7-FulR cells (Fig. 5C and D). The levels of members of the cleaved caspase family, such as PARP and caspase-3, 7, 8, 9 were all increased in MCF7-TamR and MCF7-FulR cells co-treated with NM and PAL (Fig. 5E). The mitochondria membrane potential was further used to evaluate the effect of combinational treatment of NM and PAL on apoptosis of MCF7-TamR and MCF7-FulR cells. Depolarization of MMP was synergistically increased by the combined NM and PAL treatment in MCF7-TamR and MCF7-FulR cells (Fig. 5F and G). Moreover, combinational treatment of NM and PAL significantly increased the expressions of Bim and BAX and decreased the levels of Bcl-2 and Bcl-XL in MCF7-TamR and MCF7-FulR cells (Fig. 5H). The effect of the combined NM and PAL treatment on the metastasis of endocrine-resistant ERPBC was further estimated. The migration and invasive activities of MCF7-TamR and MCF7-FulR cells were reduced by the combination treatment of NM and PAL (Fig. 6A–D). Besides, the combined treatment of NM and PAL also reversed EMT in the MCF7-TamR and MCF7-FulR cells (Fig. 6E)

Enhanced epigenetic repression of CDK4 and CDK6 by combinational treatment of nafamostat mesylate and palbociclib in endocrine-resistant ERPBCs

Since NM causes apoptosis and suppresses metastasis of endocrine-resistant ERPBCs via epigenetic repression of CDK4 and CDK6, the level of CDK4 and CDK6 proteins was evaluated in MCF7-TamR and MCF7-FulR cells under the combined NM and PAL treatment. The levels of CDK4 and CDK6 proteins were all decreased in MCF7-TamR and MCF7-FulR cells co-treated with NM and PAL (Fig. 7A). Moreover, the combination treatment of NM and PAL significantly reduced the mRNA levels of CDK4 and CDK6 in MCF7-TamR and MCF7-FulR cells (Fig. 7C). The acetylated K9, K27, and K56 of Histone 3 were further estimated in MCF7-TamR and MCF7-FulR cells co-treated with NM and PAL, only K27 acetylation of histone 3 was significantly decreased in MCF7-TamR and MCF7-FulR cells co-treated with NM and PAL (Fig. 7B).

Nafamostat mesylate exhibited significant therapeutic activity in orthotopic breast cancer mouse models

We subcutaneously injected endocrine-resistant ERPBC cells into Nonobese diabetic-severe combined immunodeficiency (NOD-SCID) mice. On Day 32, these mice were intraperitoneally injected with NM (30 mg/kg) or saline three times a week (Fig. 8A). The tumor volumes following treatment with 30 mg/kg NM were significantly decreased in comparison with control mice (Fig. 8B and C). Even though the tumors of MCF7-TamR and -FulR xenograft models had different growth rates. The tumor disappeared in MCF7-TamR and -FulR xenograft model mice

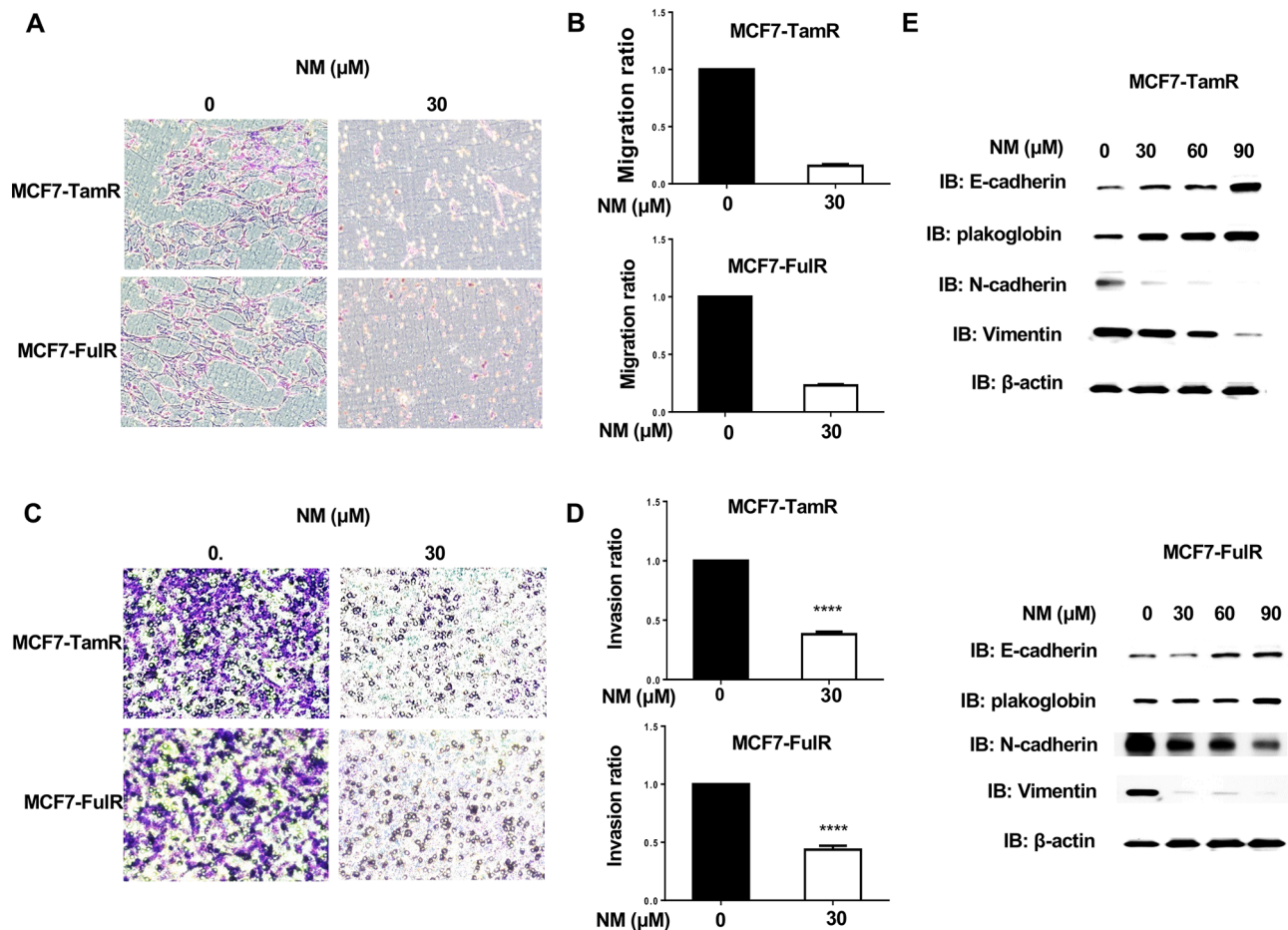


Fig. 3. Suppressive effect of nafamostat mesylate on metastasis of endocrine-resistant estrogen receptor-positive breast cancer. (A) Analysis of migration activity of MCF7-TamR (upper) and FulR (lower) cells treated with 30 μM of NM by *in vitro* Transwell-dependent migration assay. (B) Quantitative analysis of migration activity of NM-treated MCF7-TamR (upper) and FulR (lower) cells (C) Analysis of the invasive activity of MCF7-TamR (upper) and FulR (lower) cells treated with 30 μM of NM, assessed using *in vitro* invasive assays. (D) Quantitative analysis of the invasive activity of NM-treated MCF7-TamR (upper) and FulR (lower) cells. (E) Levels of markers for epithelial-mesenchymal transition in MCF7-TamR (upper) and MCF7-FulR (lower) cells treated with serial doses of NM, assessed using western blot analysis with specific antibodies. Data are represented as the mean \pm SEM for biological triplicate experiments. * $P < 0.01$, compared with the results for untreated MCF7-FulR and MCF7-TamR cells.

treated with NM. The administration of NM at 30 mg/kg did not produce observable toxic effects on the mice, and the body weights were not decreased compared to the control group (Fig. 8D). Immunohistochemistry staining (IHC) also confirmed the reduced levels of CDK4 and CDK6, which were regulated by NM (Fig. 8E), and we further calculated the percentage of nucleus staining (Fig. 8F). We found that NM not only decreased tumor size but inhibited the expression of CDK4 and CDK6. Taken together, these results suggested that NM has a valid therapeutic activity in xenograft models.

Discussion

The deprivation of estrogen signaling caused by the use of anti-hormone therapies, such as SERDs and selective ER modulators (SERMs), is the keystone of adjuvant treatment in ER-positive disease. Earlier studies have shown that endocrine therapies significantly reduce recurrence and mortality rates [3]. However, close to 30% of patients with the early-stage disease will go on to relapse with the metastatic disease following endocrine therapies, and these patients are at risk of poorer overall survival and have limited treatment options [25].

The present study investigated the antitumor and antimetastatic effects of nafamostat mesylate (NM) in endocrine-resistant ERPBC cell lines. The IC_{50} of NM was lower in the endocrine-resistant ERPBC cell lines than in the normal breast and parental breast cancer cell lines,

indicating that endocrine-resistant ERPBC cells have more sensitivity to NM than ERPBC cells. The malignancy and associated lethality of the cancer cells might be attributable to their invasiveness and metastatic mobility, in addition to their uncontrolled growth. Previous reports have demonstrated that endocrine-resistant ERPBCs are highly motile [26]. In the current investigation, treatment with NM decreased the motility of endocrine-resistant ERPBC cell lines in a dose-dependent manner. The epithelial-mesenchymal transition (EMT) plays an essential role in cancer invasion and metastasis. In the present study, we analyzed the protein levels of the EMT-associated factors N-cadherin, vimentin, E-cadherin, and β -catenin. Our results indicated that NM inhibited the metastasis of endocrine-resistant ERPBCs by enhancing the expression of E-cadherin and suppressing the levels of N-cadherin. This phenomenon has been described as a cadherin switch, and has been associated with enhanced migratory and invasive traits, which result in poorer survival in BC patients [27].

We demonstrated that NM selectively downregulated the expression of CDK4 and CDK6 at the protein and mRNA levels in MCF7-TamR and MCF7-FulR cancer cells. These observations suggested that the antitumor effect of NM has an excellent kinase selectivity profile. These issues have been overcome by the use of far more specific inhibitors, that target CDK4 and CDK6, such as PAL, ribociclib, and abemaciclib. The addition of CDK4/6 inhibitors that target the cell cycle machinery and EMT has significantly improved the outcomes of advanced ER+ breast

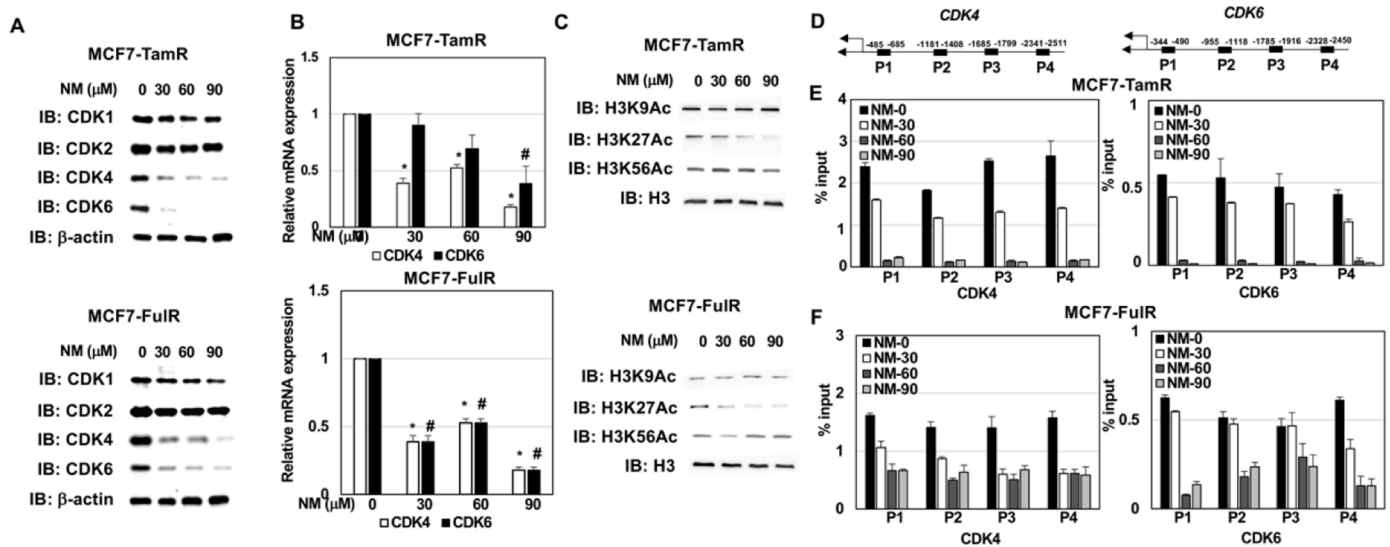


Fig. 4. Epigenetic repression of CDK4 and CDK6 expression induced by nafamostat mesylate in endocrine-resistant estrogen receptor-positive breast cancer cells. (A) Levels of CDK families in MCF7-TamR (upper) and -FuIR (lower) cells treated with a serial dose of NM, assessed using western blot analysis with specific antibodies. (B) mRNA levels of CDK4 and CDK6 in MCF7-TamR (upper) and -FuIR (lower) cells treated with serial doses of NM, assessed using quantitative PCR assay. (C) Acetylation levels of histone 3 in MCF7-TamR (upper) and -FuIR (lower) cells treated with serial doses of NM, assessed using western blot analysis with specific antibodies. (D) A simple diagram for the P1, P2, P3, and P4 regions of CDK4 (left) and CDK6 (right). (E) Binding levels of Histone 3 Lysine 27 at the promoter region of CDK4 in MCF7-TamR (left) and -FuIR (right) cells treated with serial doses of NM, assessed using qChIP-PCR assays. (F) Binding levels of Histone 3 Lysine 27 at the promoter region of CDK6 in MCF7-TamR (left) and -FuIR (right) cells treated with serial doses of NM, assessed using qChIP-PCR assay. Data are represented as the mean \pm SEM for biological triplicate experiments. $^{*}P < 0.01$, compared with the results for untreated MCF7-FuIR and MCF7-TamR cells.

cancers. In particular, PAL has demonstrated significant benefits in Phase II and III clinical trials (PALOMA-1, -2 and -3), doubling the progression-free survival (PFS) compared to letrozole or fulvestrant alone [28,29]. A recent meta-analysis of nine studies also demonstrated that treatment with CDK 4/6 inhibitors plus endocrine therapy improved overall survival, PFS, and objective response rate among patients with HR-positive, ERBB2-negative metastatic BC [30]. However, there were several patients who did not respond to PAL, experiencing disease progression within 24 weeks, or developing clinical resistance within 25 months after the initiation of treatment [31]. Adverse effects such as neutropenia and leukopenia may result in discontinuation or interruption of treatment, hence reducing the therapeutic benefits. All-grade neutropenia was reported in approximately 80% of the overall population in the PAL arms of both PALOMA-2 and PALOMA-3 [29]. The significant myelotoxicity of PAL has led to dose interruption, and the drug is administered on a three-week-on/one-week-off schedule, to allow marrow recovery. This interrupted dosing offers the possibility of potent synergy using combination therapies with drugs acting on other aspects of the cell cycle. In the current study, we first demonstrated that NM induced apoptosis of endocrine-resistant ERPBC cells alone. We then used combinational treatment with NM and PAL, showing that the enhanced cooperation of both agents induced apoptosis and suppressed metastasis of endocrine-resistant ERPBC cells. This result indicated that NM might potentiate the activity of CDK4/6 inhibitors for the treatment of endocrine-resistant ERPBC cells. It also implied that NM may be used with DK4/6 inhibitors in an alternative dosing strategy during the one-week-off schedule.

Our study also provided insight into the molecular mechanism whereby NM induces apoptosis and suppresses metastasis in endocrine-resistant ERPBC via epigenetic modification of CDK4/6 expression and regulation of H3K27. NM is a synthetic serine protease inhibitor clinically used for patients with pancreatitis, disseminated intravascular coagulation, and systematic inflammatory response syndrome [9,10]. Previous studies have demonstrated the inhibitory effect of NM on nuclear factor kappa-B (NF- κ B) signaling to induce apoptosis and inhibit cell adhesion and invasion in various cancer cell lines [11,12,32]. In the present study, we examined the anti-cancer activity of NM against

endocrine-resistant ERPBC cell lines. Our results indicated that NM reduced CDK4/6 expression via the epigenetic downregulation of H3K27Ac. It is possible that NM inhibited CDK4/6 expression via the NF- κ B signaling pathway, as NF- κ B reportedly regulates H3K27Ac and controls genome-wide activation at the promoters and enhancers of the targeted genes [33]. NF- κ B recruits CBP to activate downstream target gene expression [34]. The p65 expression was repressed by NM [12]. Taken together, CBP is a potential effector in epigenetic repression of CDK4 and CDK6 in NM-treated endocrine-resistant ERPBCs via the decreased binding level of H3K27Ac. Future studies should aim to analyze the interplay of the NF- κ B signaling pathway and endocrine-resistant ERPBC at the level of chromatin, considering the different mechanisms involved in the development of resistance to endocrine treatment.

Conclusions

Collectively, our data demonstrated a previously unreported consequence of employing NM in endocrine-resistant ERPBC. First, NM induced apoptosis and inhibited the metastasis of endocrine-resistant ERPBC cells. Second, NM inhibited CDK4/6 expression via epigenetic regulation of H3K27, whose levels were decreased in a dose-dependent manner. Our results specifically clarified the way in which NM acts as an anti-cancer drug for endocrine-resistant ERPBC, by elucidating the relationship between signal transduction and epigenetic regulation. Enhanced inhibition of endocrine-resistant ERPBC caused by combination treatment with CDK4/6 inhibitor and NM is a potential strategy for use in clinical medicine. These findings provided insights into the potential of utilizing NM for the treatment of estrogen-resistant ERPBC.

Funding

This work was supported to H.T.W. by the Ministry of Science and Technology Summit Grant (MOST 110-2314-B-371-007-MY3) and Changhua Christian Hospital (110-CCH-IRP-033); Y.T.L. by the Ministry of Science and Technology Summit Grant MOST 110-2314-B-182A-011)

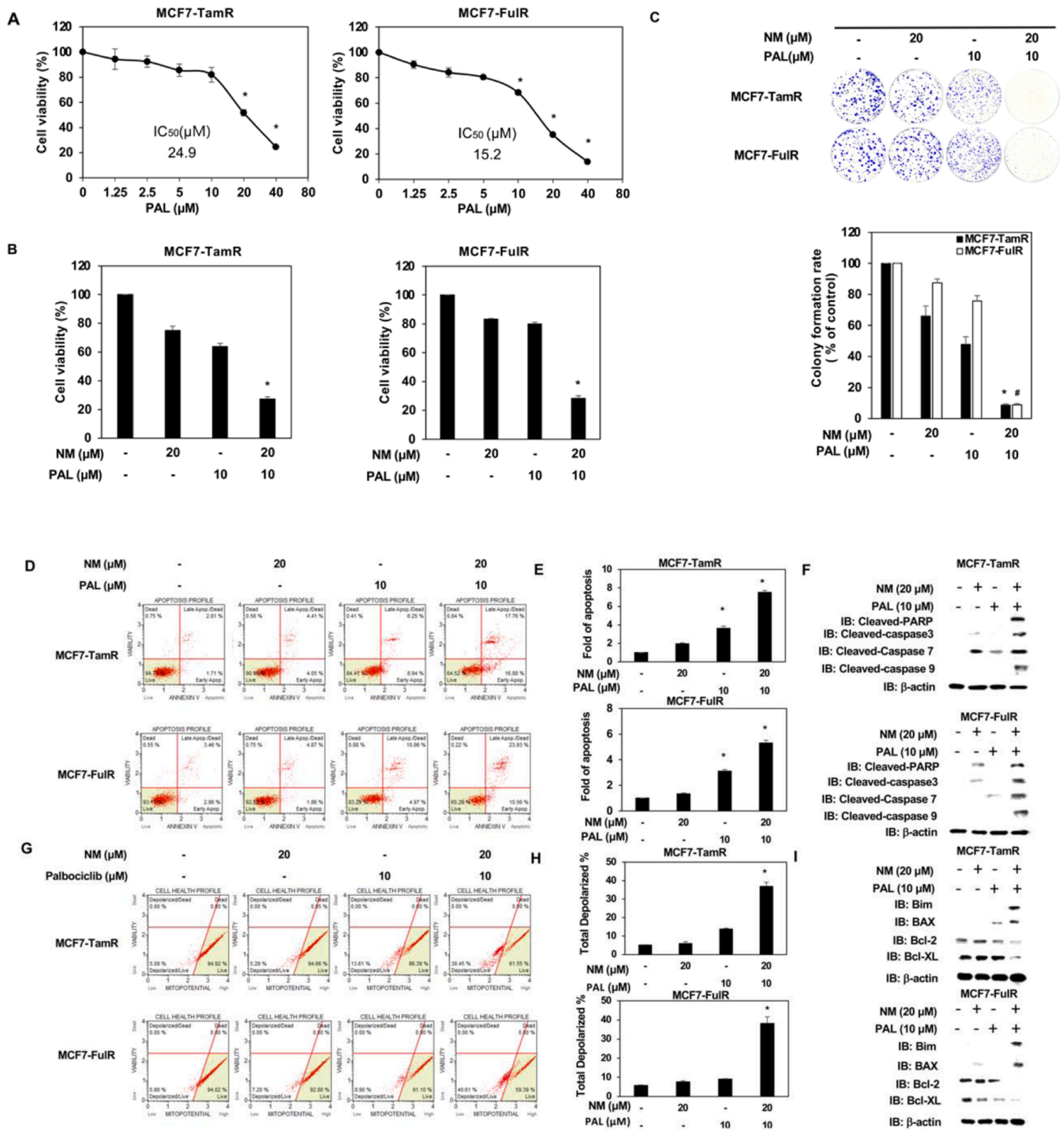


Fig. 5. Effect of the combined nafamostat mesylate and PAL on apoptosis of endocrine-resistant estrogen receptor-positive breast cancer. (A) IC₅₀ value of MCF7-TamR (left) and -FuIR (right) cells for PAL, assessed using MTT assay. (B) Analysis of cell viability of MCF7-TamR (left) and -FuIR (right) cells under combined NM and PAL treatment, assessed using MTT assays. (C) Analysis of apoptotic levels of MCF7-TamR (upper) and -FuIR (lower) cells under combined NM and PAL treatment, assessed using Annexin V-dependent flow cytometry assays. (D) Quantitative analysis of apoptosis in combined NM and PAL treated-MCF7-TamR (upper) and -FuIR (lower) cells. (E) Levels of cleaved caspase families in MCF7-TamR (upper) and -FuIR (lower) cells under combined NM and PAL treatment, assessed using western blotting analysis with specific antibodies. (F) Analysis of mitochondrial membrane potential of MCF7-TamR (upper) and MCF7-FuIR (lower) cells under combined NM and PAL treatment, assessed using flow cytometry assays. (G) Quantitative analysis of total depolarized levels of combined NM and PAL-treated MCF7-TamR (upper) and FuIR (lower) cells. (H) Levels of BCL families and death signaling-related proteins in MCF7-TamR (upper) and FuIR (lower) cells under serial doses of NM, assessed using western blot analysis with specific antibodies. Data are represented as the mean ± SEM of biological triplicate experiments. ^{*}*P* < 0.01, compared with the results for untreated MCF7-FuIR and MCF7-TamR cells.

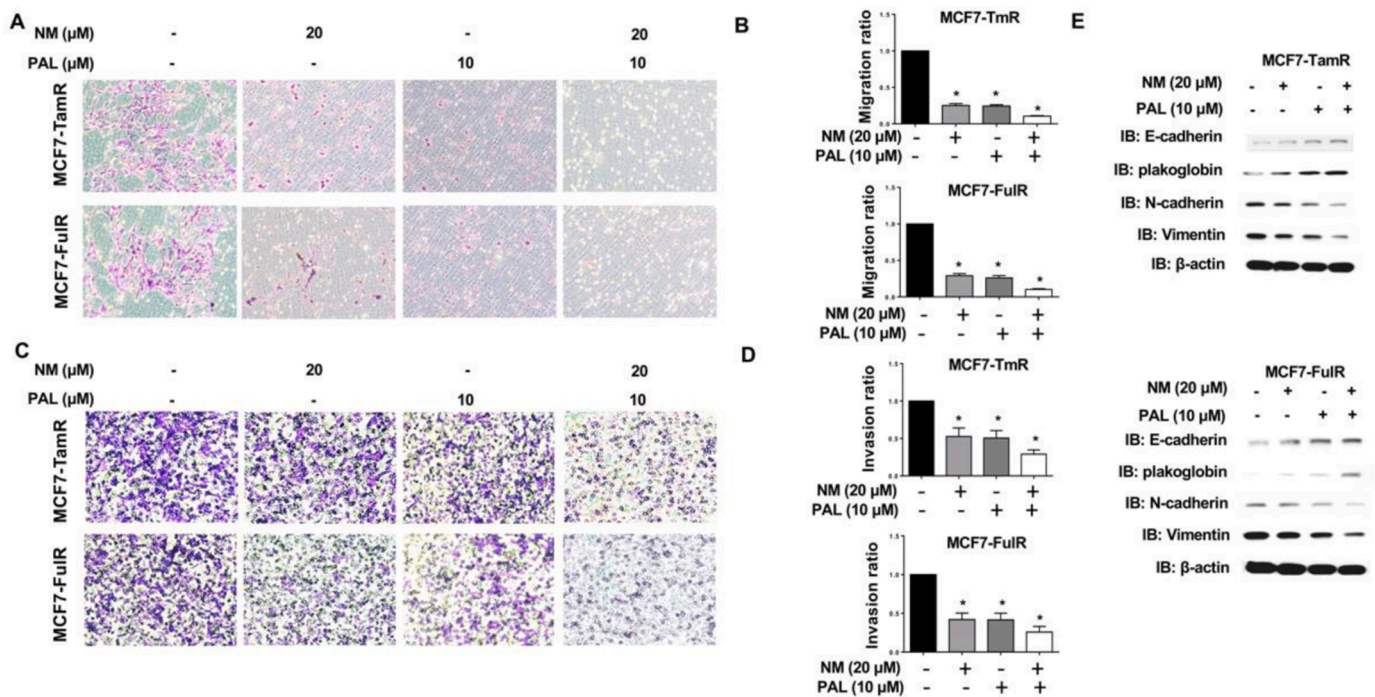


Fig. 6. Enhanced suppression of combined nafenostat mesylate and PAL on the metastasis of endocrine-resistant estrogen receptor-positive breast cancer. (A) Effect of NM and PAL on the migration activity of MCF7-TamR (upper) and MCF7-FuIR (lower) cells, assessed using *in vitro* migration assays. (B) Quantitative analysis of the migration activity of MCF7-TamR (upper) and MCF7-FuIR (lower) cells under NM and PAL treatment. (C) Effect of combined NM and PAL on the invasive activity of MCF7-TamR (upper panel) and MCF7-FuIR (lower) cells, assessed using *in vitro* invasion assays. (D) Quantitative analysis of the invasive activity of MCF7-TamR (upper) and MCF7-FuIR (lower) cells under NM and PAL treatment. (E) Levels of markers for the epithelial-mesenchymal transition in MCF7-TamR (upper) and MCF7-FuIR (lower) cells treated with a combination of NM and PAL, assessed using western blot analysis with specific antibodies. Data are represented as the mean ± SEM for biological triplicate experiments. **P* < 0.01, compared with the results for untreated MCF7-FuIR and MCF7-TamR cells.

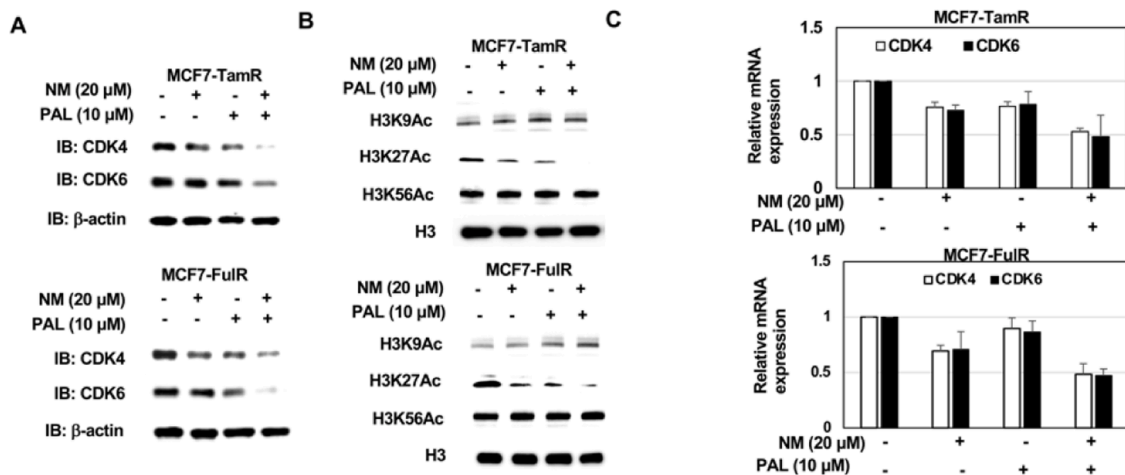
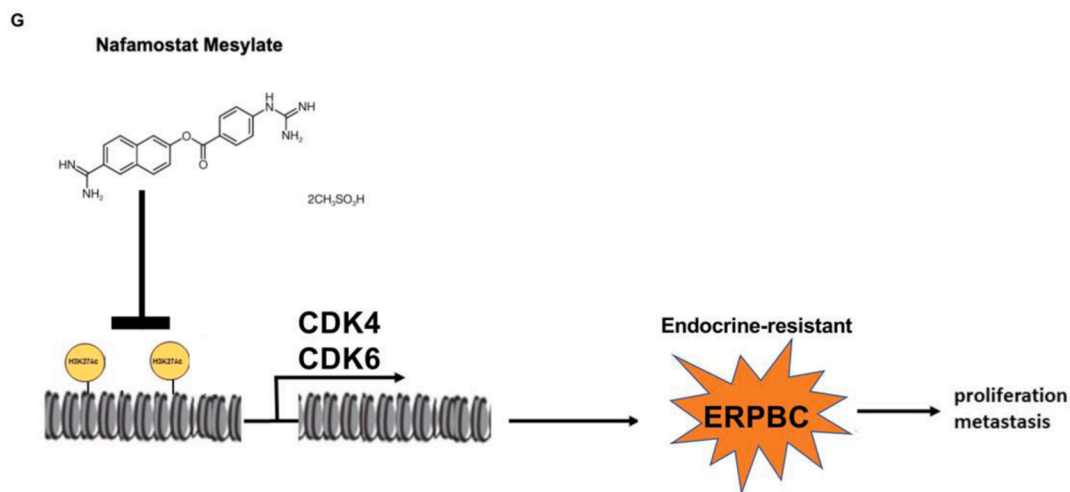
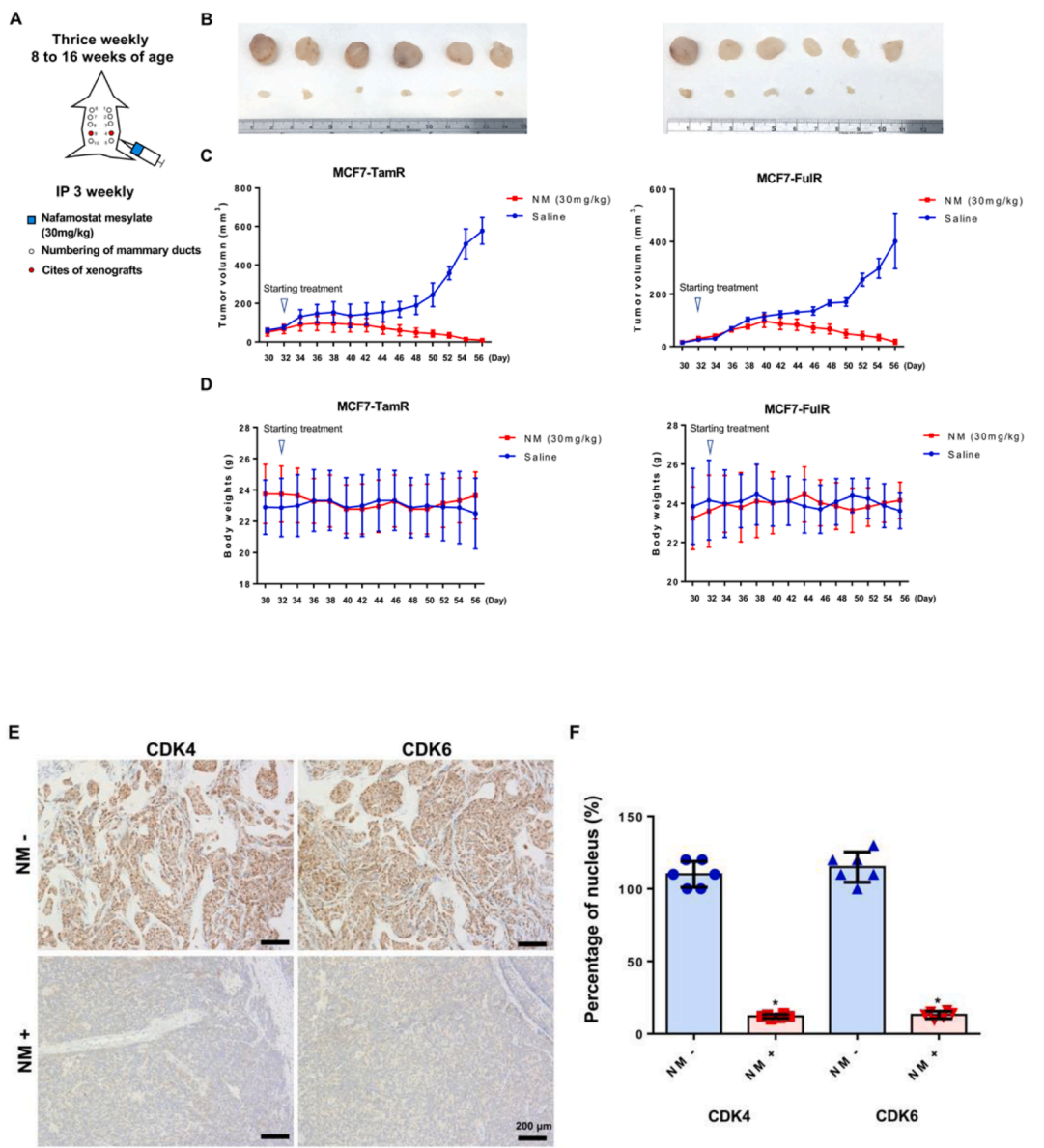


Fig. 7. Epigenetic repression of combined nafenostat mesylate and PAL on CDK4/6 expression in endocrine-resistant estrogen receptor-positive breast cancer cells. (A) Levels of CDK4 and CDK6 expression in combined NM and PAL-treated MCF7-TamR (upper) and MCF7-FuIR (lower) cells, assessed using western blot analysis with specific antibodies. (B) mRNA levels of CDK4 and CDK6 in MCF7-TamR (upper) and MCF7-FuIR (upper) cells treated with NM and PAL, assessed using quantitative PRC analysis. (C) Levels of Histone 3 modification in MCF7-TamR (upper) and MCF7-FuIR (lower) cells treated with NM and PAL, assessed using western blot analysis with specific antibodies. Data are represented as the mean ± SEM for biological triplicate experiments. **P* < 0.01, compared with the results for untreated MCF7-FuIR and MCF7-TamR cells.

CRediT authorship contribution statement

Yueh-Te Lin: Conceptualization, Visualization, Funding acquisition, Formal analysis, Data curation. **Joseph Lin:** Conceptualization, Visualization. **Yi-En Liu:** Funding acquisition, Formal analysis, Data curation. **Kai-Wen Hsu:** Funding acquisition, Formal analysis, Data curation. **Chang-Chi Hsieh:** Funding acquisition, Formal analysis, Data

curation. **Dar-Ren Chen:** Writing – original draft, Writing – review & editing. **Han-Tsang Wu:** Conceptualization, Visualization, Funding acquisition, Formal analysis, Data curation, Writing – original draft, Writing – review & editing.



(caption on next page)

Fig. 8. Inhibitory effect of NM on endocrine-resistant ERPCB in xenograft models and a model to summarize the results. (A) Eight-week-old female SCID mice were inoculated with MCF7-TemR and MCF7-FuIR cells orthotopically. On Day 32, mice were injected with saline and nafamostat mesylate (30 mg/kg) three times a week, intraperitoneally. (B) Nafamostat mesylate significantly decreased tumor growth. The tumor sizes were measured at Day 56. The upper tumors are the control groups and the lower are nafamostat mesylate treatment. (C) Tumor progression was time-dependent. (D) The body weights were not significantly different between the control and nafamostat mesylate treatment groups. (E) Nafamostat mesylate significantly reduced expressions of CDK4 and CDK6 by immunohistochemistry stain analysis. Scale bars represented 200 μ m. (F) Decreased nucleus staining in the Nafamostat mesylate-treated mice. There is a statistical significance between control and nafamostat mesylate-treated mice (* $P < 0.001$). Six mice were used for each group. (G) A model to summarize the results of this report.

Declaration of Competing Interest

There is no conflict of interest.

Acknowledgments

We thank Y.C.C and H.T.L. at Changhua Christian Hospital for experimental assistance in this study.

Supplementary materials

Supplementary material associated with this article can be found, in the online version, at doi:10.1016/j.tranon.2021.101302.

References

- M.E.H. Hammond, D.F. Hayes, M. Dowsett, D.C. Allred, K.L. Hagerty, S. Badve, P. L. Fitzgibbons, G. Francis, N.S. Goldstein, M. Hayes, American society of clinical oncology/college of American pathologists guideline recommendations for immunohistochemical testing of estrogen and progesterone receptors in breast cancer (unabridged version), *Arch. Pathol. Lab. Med.* 134 (2010) e48–e72. K.H. Allison, M.E.H. Hammond, M. Dowsett, S.E. McKernin, L.A. Carey, P.L. Fitzgibbons, D.F. Hayes, S.R. Lakhani, M. Chavez-MacGregor, J. Perlmutter, Estrogen and progesterone receptor testing in breast cancer: American Society of Clinical Oncology/College of American Pathologists guideline update, *Archives of pathology & laboratory medicine*, 144 (2020) 545–563.
- M. Colleoni, S. Gelber, A.S. Coates, M. Castiglione-Gertsch, R.D. Gelber, K. Price, C. M. Rudenstam, J. Lindtner, J. Collins, B. Thürlimann, Influence of endocrine-related factors on response to perioperative chemotherapy for patients with node-negative breast cancer, *J. Clin. Oncol.* 19 (2001) 4141–4149.
- N.U. Lin, E.P. Winer, Advances in adjuvant endocrine therapy for postmenopausal women, *J. Clin. Oncol.* 26 (2008) 798–805.
- L. Piggott, A. Silva, T. Robinson, A. Santiago-Gómez, B.M. Simões, M. Becker, I. Fichtner, L. Andera, P. Young, C. Morris, Acquired resistance of ER-positive breast cancer to endocrine treatment confers an adaptive sensitivity to TRAIL through posttranslational downregulation of c-FLIP, *Clin. Cancer Res.* 24 (2018) 2452–2463.
- H. Pan, R. Gray, J. Braybrooke, C. Davies, C. Taylor, P. McGale, R. Peto, K. I. Pritchard, J. Bergh, M. Dowsett, 20-year risks of breast-cancer recurrence after stopping endocrine therapy at 5 years, *New Engl. J. Med.* 377 (2017) 1836–1846.
- C.G. Murphy, M.N. Dickler, Endocrine resistance in hormone-responsive breast cancer: mechanisms and therapeutic strategies, *Endocr. Relat. Cancer* 23 (2016) R337–R352.
- W. Toy, Y. Shen, H. Won, B. Green, R.A. Sakr, M. Will, Z. Li, K. Gala, S. Fanning, T. A. King, ESR1 ligand-binding domain mutations in hormone-resistant breast cancer, *Nat. Genet.* 45 (2013) 1439–1445.
- J.F. Robertson, I.M. Bondarenko, E. Trishkina, M. Dvorkin, L. Panasci, A. Manikhas, Y. Shparyk, S. Cardona-Huerta, K.L. Cheung, M.J. Philco-Salas, Fulvestrant 500mg versus anastrozole 1mg for hormone receptor-positive advanced breast cancer (FALCON): an international, randomised, double-blind, phase 3 trial, *Lancet* 388 (2016) 2997–3005.
- C.C. Lin, L.J. Lin, S.D. Wang, C.J. Chiang, Y.P. Chao, J. Lin, S.T. Kao, The effect of serine protease inhibitors on airway inflammation in a chronic allergen-induced asthma mouse model, *Mediat. Inflamm.* 2014 (2014), 879326, 10 pages.
- E.Y. Cho, S.C. Choi, S.H. Lee, J.Y. Ahn, L.R. Im, J.H. Kim, M. Xin, S.U. Kwon, D. K. Kim, Y.M. Lee, Nafamostat mesilate attenuates colonic inflammation and mast cell infiltration in the experimental colitis, *Int. Immunopharmacol.* 11 (2011) 412–417. S. Noguchi, M. Nakatsuka, H. Konishi, Y. Kamada, C. Chekir, T. Kudo, Nafamostat mesilate suppresses NF- κ B activation and NO overproduction in LPS-treated macrophages, *International immunopharmacology*, 3 (2003) 1335–1344.
- T. Uwagawa, Z. Li, Z. Chang, Q. Xia, B. Peng, G.M. Sclabas, S. Ishiyama, M.C. Hung, D.B. Evans, J.L. Abbruzzese, Mechanisms of synthetic serine protease inhibitor (FUT-175)-mediated cell death, *Cancer Interdiscip. Int. J. Am. Cancer Soc.* 109 (2007) 2142–2153.
- Y. Fujiwara, K. Furukawa, K. Haruki, Y. Shimada, T. Iida, H. Shiba, T. Uwagawa, T. Ohashi, K. Yanaga, Nafamostat mesilate can prevent adhesion, invasion and peritoneal dissemination of pancreatic cancer thorough nuclear factor kappa-B inhibition, *J. Hepatobiliary Pancreat. Sci.* 18 (2011) 731–739.
- S. Mander, D.J. You, S. Park, D.H. Kim, H.J. Yong, D.S. Kim, C. Ahn, Y.H. Kim, J. Y. Seong, J.I. Hwang, Nafamostat mesilate negatively regulates the metastasis of triple-negative breast cancer cells, *Arch. Pharm. Res.* 41 (2018) 229–242.
- X. Chen, Z. Xu, S. Zeng, X. Wang, W. Liu, L. Qian, J. Wei, X. Yang, Q. Shen, Z. Gong, The molecular aspect of antitumor effects of protease inhibitor nafamostat mesylate and its role in potential clinical applications, *Front. Oncol.* 9 (2019) 852. S. Homma, K. Hayashi, K. Yoshida, Y. Sagawa, Y. Kamata, M. Ito, Nafamostat mesilate, a serine protease inhibitor, suppresses interferon-gamma-induced up-regulation of programmed cell death ligand 1 in human cancer cells, *International immunopharmacology*, 54 (2018) 39–45.
- H.T. Wu, J. Lin, Y.E. Liu, H.F. Chen, K.W. Hsu, S.H. Lin, K.Y. Peng, K.J. Lin, C. C. Hsieh, D.R. Chen, Luteolin suppresses androgen receptor-positive triple-negative breast cancer cell proliferation and metastasis by epigenetic regulation of MMP9 expression via the AKT/mTOR signaling pathway, *Phytomedicine* 81 (2021), 153437.
- M. Labrie, Y. St-Pierre, Epigenetic regulation of mmp-9 gene expression, *Cell. Mol. life Sci.* 70 (2013) 3109–3124.
- S. Attoub, A.H. Hassan, B. Vanhoecque, R. Iratni, T. Takahashi, A.M. Gaben, M. Bracke, S. Awad, A. John, H.A. Kamalboor, Inhibition of cell survival, invasion, tumor growth and histone deacetylase activity by the dietary flavonoid luteolin in human epithelioid cancer cells, *Eur. J. Pharmacol.* 651 (2011) 18–25. E. Ceccacci, S. Minucci, Inhibition of histone deacetylases in cancer therapy: lessons from leukaemia, *British journal of cancer*, 114 (2016) 605–611.
- H.T. Wu, Y.C. Kuo, J.J. Hung, C.H. Huang, W.Y. Chen, T.Y. Chou, Y. Chen, Y. J. Chen, Y.J. Chen, W.C. Cheng, S.C. Teng, K.J. Wu, K63-polyubiquitinated HAUSP deubiquitinates HIF-1 α and dictates H3K56 acetylation promoting hypoxia-induced tumour progression, *Nat. Commun.* 7 (2016) 13644.
- M. Nikolaou, A. Pavlopoulou, A.G. Georgakilas, E. Kyrodimos, The challenge of drug resistance in cancer treatment: a current overview, *Clin. Exp. Metastasis* 35 (2018) 309–318.
- M. Roberto, A. Astone, A. Botticelli, L. Carboognin, A. Cassano, G. D'Auria, A. Fabbri, A. Fabi, T. Gamucci, E. Krasniqi, CDK4/6 inhibitor treatments in patients with hormone receptor positive, Her2 negative advanced breast cancer: potential molecular mechanisms, clinical implications and future perspectives, *Cancers (Basel)* 13 (2021) 332.
- H. Mamiya, R. Tahara, S. Tolaney, N. Choudhry, M. Najafzadeh, Cost-effectiveness of palbociclib in hormone receptor-positive advanced breast cancer, *Ann. Oncol.* 28 (2017) 1825–1831.
- P. Guo, W. Chen, H. Li, M. Li, L. Li, The histone acetylation modifications of breast cancer and their therapeutic implications, *Pathol. Oncol. Res.* 24 (2018) 807–813.
- T. Liu, J. Yu, M. Deng, Y. Yin, H. Zhang, K. Luo, B. Qin, Y. Li, C. Wu, T. Ren, CDK4/6-dependent activation of DUB3 regulates cancer metastasis through SNAI1, *Nat. Commun.* 8 (2017) 1–12. Z. Zhang, J. Li, Y. Ou, G. Yang, K. Deng, Q. Wang, Z. Wang, W. Wang, Q. Zhang, H. Wang, CDK4/6 inhibition blocks cancer metastasis through a USP51-ZEB1-dependent deubiquitination mechanism, *Signal transduction and targeted therapy*, 5 (2020) 1–13.
- A. Lee, M.B. Djamgoz, Triple negative breast cancer: emerging therapeutic modalities and novel combination therapies, *Cancer Treat. Rev.* 62 (2018) 110–122. R.B. Mokhtari, T.S. Homayouni, N. Baluch, E. Morgatskaya, S. Kumar, B. Das, H. Yeger, Combination therapy in combating cancer, *Oncotarget*, 8 (2017) 38022.
- T. Reinert, C.H. Barrios, Optimal management of hormone receptor positive metastatic breast cancer in 2016, *Ther. Adv. Med. Oncol.* 7 (2015) 304–320.
- S. Hiscox, L. Morgan, D. Barrow, C. Dutkowski, A. Wakeling, R.I. Nicholson, Tamoxifen resistance in breast cancer cells is accompanied by an enhanced motile and invasive phenotype: inhibition by gefitinib (Iressa[®], ZD1839), *Clin. Exp. Metastasis* 21 (2004) 201–212. B.C. Browne, F. Hochgräfe, J. Wu, E.K. Millar, J. Barraclough, A. Stone, R.A. McCloy, C.S. Lee, C. Roberts, N.A. Ali, Global characterization of signalling networks associated with tamoxifen resistance in breast cancer, *The FEBS journal*, 280 (2013) 5237–5257.
- M.A. Aleskandarany, O.H. Negm, A.R. Green, M.A. Ahmed, C.C. Nolan, P.J. Tighe, I.O. Ellis, E.A. Rakha, Epithelial mesenchymal transition in early invasive breast cancer: an immunohistochemical and reverse phase protein array study, *Breast Cancer Res. Treat.* 145 (2014) 339–348.
- R.S. Finn, J.P. Crown, I. Lang, K. Boer, I.M. Bondarenko, S.O. Kulyk, J. Ettl, R. Patel, T. Pinter, M. Schmidt, The cyclin-dependent kinase 4/6 inhibitor palbociclib in combination with letrozole versus letrozole alone as first-line treatment of oestrogen receptor-positive, HER2-negative, advanced breast cancer (PALOMA-1/TRIO-18): a randomised phase 2 study, *Lancet Oncol.* 16 (2015) 25–35.
- N.C. Turner, J. Ro, F. André, S. Loi, S. Verma, H. Iwata, N. Harbeck, S. Loibl, C. Huang Bartlett, K. Zhang, Palbociclib in hormone-receptor-positive advanced breast cancer, *New Engl. J. Med.* 373 (2015) 209–219. R.S. Finn, M. Martin, H.S. Rugo, S. Jones, S.-A. Im, K. Gelmon, N. Harbeck, O.N. Lipatov, J.M. Walshe, S. Moulder, Palbociclib and letrozole in advanced breast cancer, *New England journal of medicine*, 375 (2016) 1925–1936.
- J. Li, X. Huo, F. Zhao, D. Ren, R. Ahmad, X. Yuan, F. Du, J. Zhao, Association of cyclin-dependent kinases 4 and 6 inhibitors with survival in patients with hormone

- receptor-positive metastatic breast cancer: a systematic review and meta-analysis, *JAMA Netw. Open* 3 (2020), e2020312. -e2020312.
- [31] S. Vijayaraghavan, C. Karakas, I. Doostan, X. Chen, T. Bui, M. Yi, A. S. Raghavendra, Y. Zhao, S.I. Bashour, N.K. Ibrahim, CDK4/6 and autophagy inhibitors synergistically induce senescence in Rb positive cytoplasmic cyclin E negative cancers, *Nat. Commun.* 8 (2017) 1–17.
- [32] K. Furukawa, T. Iida, H. Shiba, Y. Fujiwara, T. Uwagawa, Y. Shimada, T. Misawa, T. Ohashi, K. Yanaga, Anti-tumor effect by inhibition of NF- κ B activation using nafamostat mesilate for pancreatic cancer in a mouse model, *Oncol. Rep.* 24 (2010) 843–850. K. Haruki, H. Shiba, Y. Fujiwara, K. Furukawa, R. Iwase, T. Uwagawa, T. Misawa, T. Ohashi, K. Yanaga, Inhibition of nuclear factor- κ B enhances the antitumor effect of tumor necrosis factor- α gene therapy for hepatocellular carcinoma in mice, *Surgery*, 154 (2013) 468–478.
- [33] L. Jurida, J. Soelch, M. Bartkuhn, K. Handschick, H. Müller, D. Newel, A. Weber, O. Dittrich-Breiholz, H. Schneider, S. Bhujju, The activation of IL-1-induced enhancers depends on TAK1 kinase activity and NF- κ B p65, *Cell Rep.* 10 (2015) 726–739.
- [34] S.P. Mukherjee, M. Behar, H.A. Birnbaum, A. Hoffmann, P.E. Wright, G. Ghosh, Analysis of the RelA: cBP/p300 interaction reveals its involvement in NF- κ B-driven transcription, *PLoS Biol.* 11 (2013), e1001647.